

Measurements in thermoacoustic oscillations :

(ii) chemiluminescence and imaging

S. Hochgreb
University of Cambridge

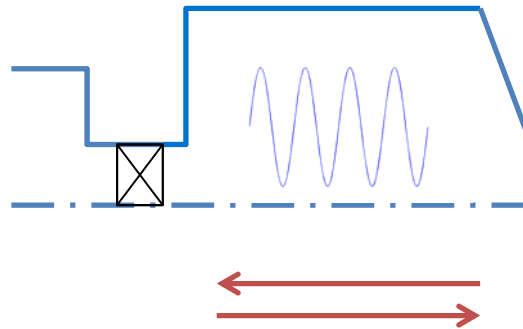
Tango Workshop
IIT Madras, 4-7 Feb, 2014

Outline

- Measurement of heat release rates
 - Direct method
 - Chemiluminescence
 - Pressure method
- Imaging measurements
 - Chemiluminescence
 - OH PLIF
 - High speed measurements
 - Phase-reconstructed measurements

Outline

- Measurement of heat release rates
 - Direct method
 - Chemiluminescence
 - Pressure method
- Imaging measurements
 - Chemiluminescence
 - OH PLIF
 - High speed measurements
 - Phase-reconstructed measurements



Take div (momentum) + D/Dt (thermodyn)

$$\frac{D^2 p'}{Dt^2} - c^2 \frac{\partial^2 p'}{\partial x^2} = \frac{\gamma - 1}{\gamma} \frac{p}{\mathcal{R}} \frac{D^2 s'}{Dt^2}$$

heat release rate/volume

Usual assumption:

$$\frac{Ds'}{Dt} = \frac{q' \leftarrow}{\rho T} = q' \frac{\mathcal{R}}{p}$$

Connect q' to p' or u'

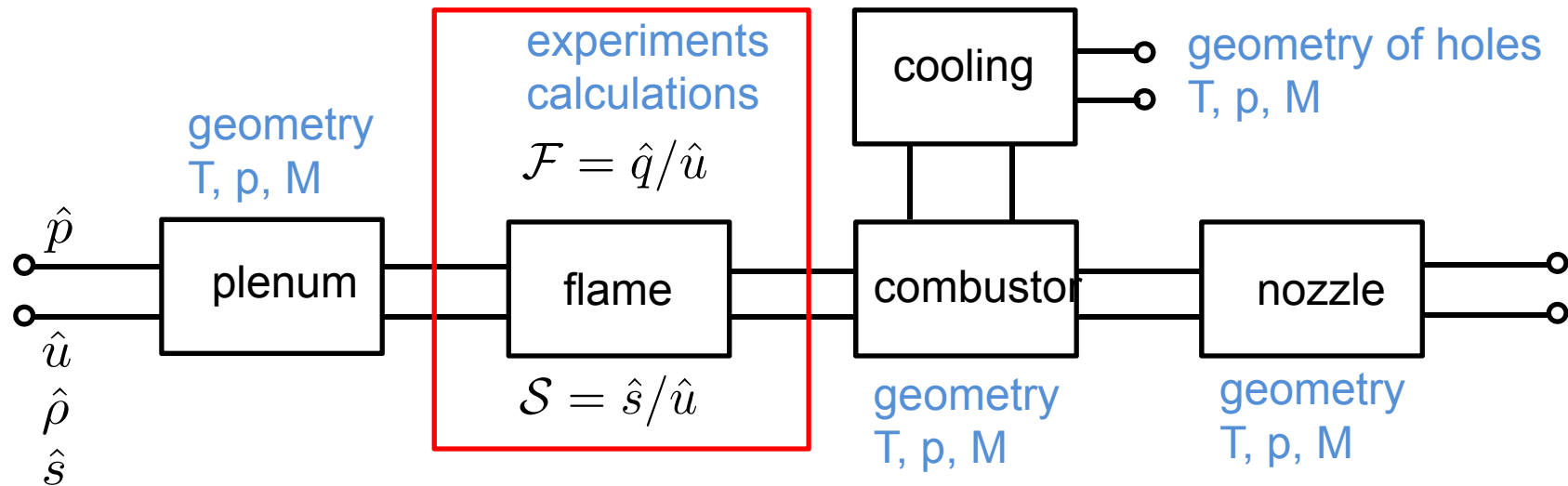
$$\frac{D^2 p'}{Dt^2} - c^2 \frac{\partial^2 p'}{\partial x^2} = \frac{\gamma - 1}{\gamma} \boxed{\frac{Dq'}{Dt}}$$

So that:

wave equation

source term

Network models

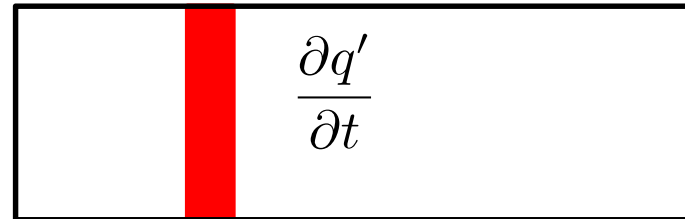


Transfer function between boxes
Coupling between state variables

Allows de-coupling between different elements
Individual model for each sub-system

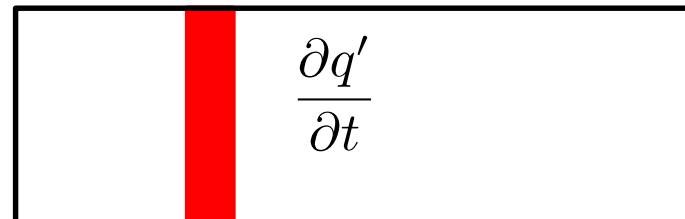
Largely most used and very successful model

Measurement of heat release rate fluctuation



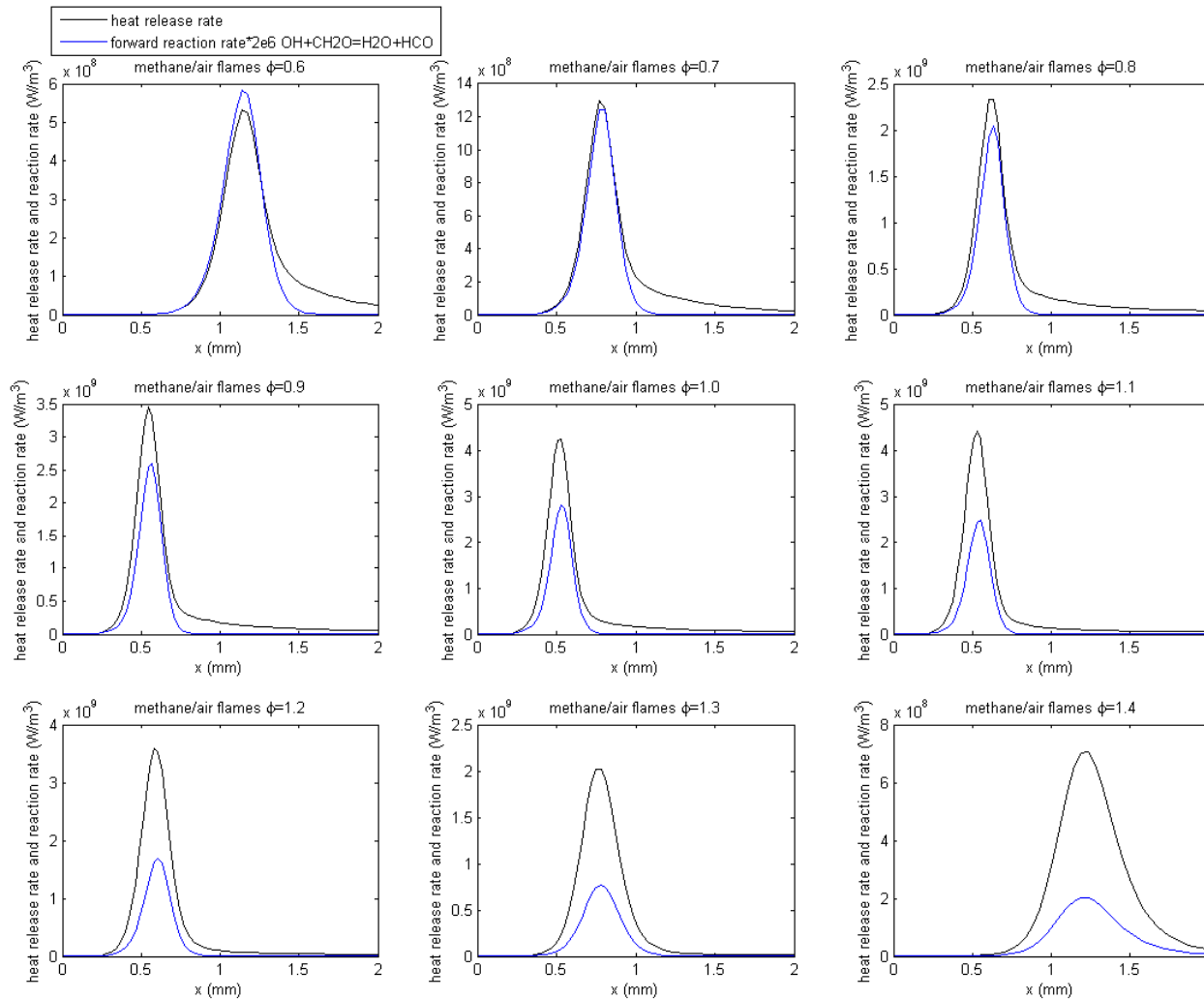
- Direct
- Chemiluminescence
- Pressure

Measurement of heat release rate fluctuation

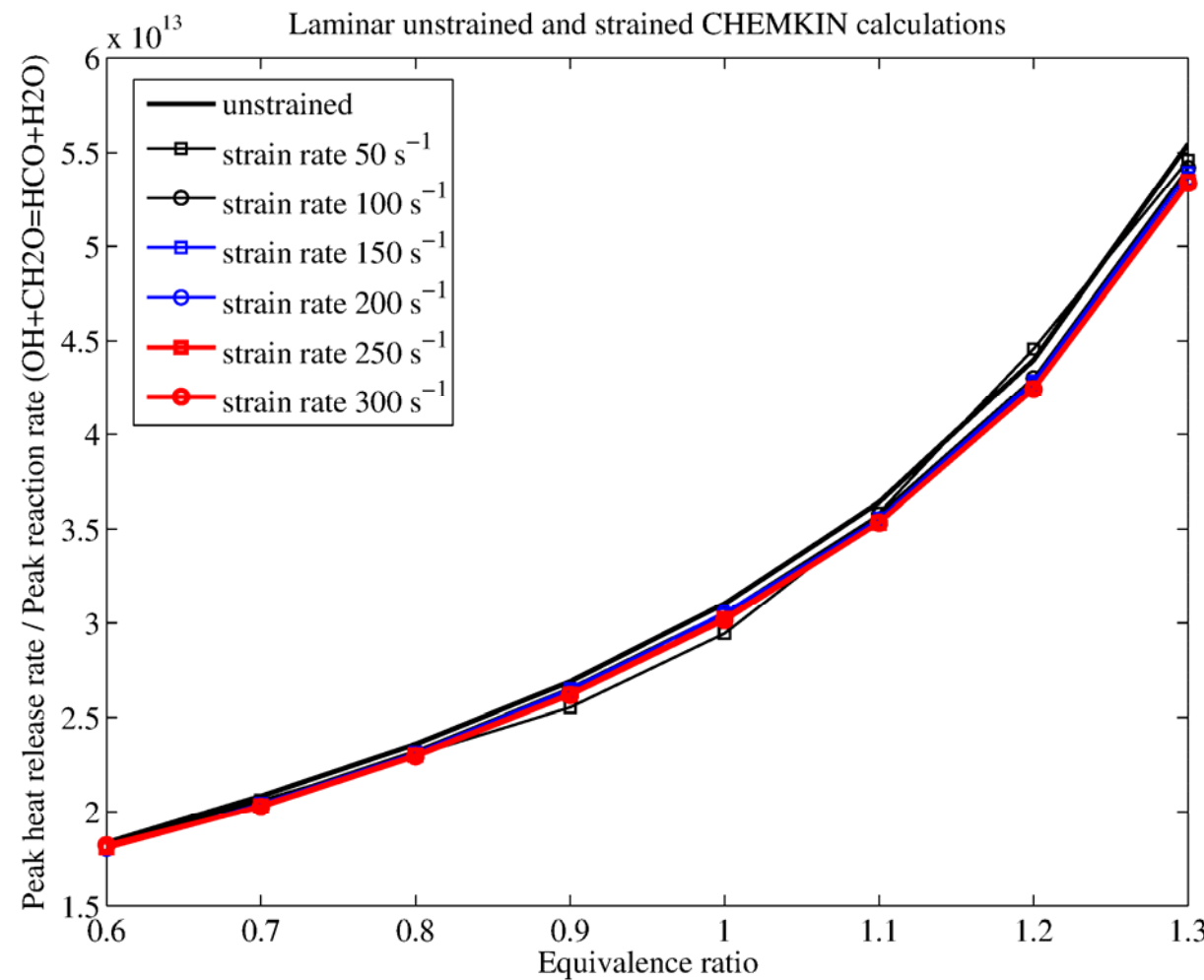


- Direct
- Chemiluminescence
- Pressure

Direct: Heat release rate in laminar methane flames



Heat release rate in methane flames



Heat release rate fluctuation

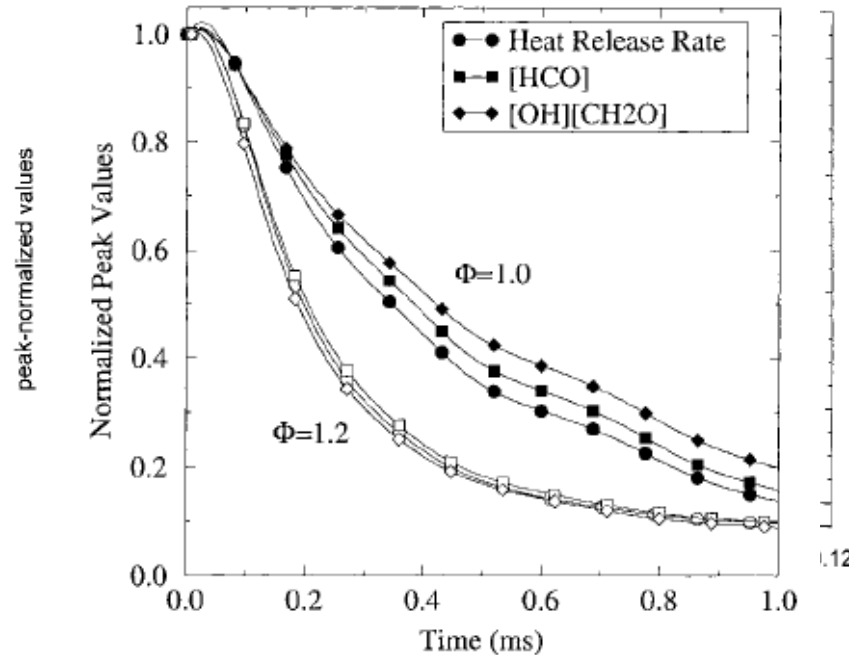


FIG. 1. Time variation of peak heat release rate, HCO concentration, and the product of OH and CH₂O concentrations. Taken on the centerline from a computed [4] 2-D counter-rotating vortex-pair colliding with a laminar premixed flame (CH₄-air, $\phi = 1$ and 1.2, 20% N₂ dilution). Values normalized to the values in the undisturbed flame.

Paul, P. H. and Najm, H. N. Proc. Comb. Inst. 27 (1998)

$q' \sim [\text{OH}][\text{CH}_2\text{O}]$
Use excitation lines with low T dependence

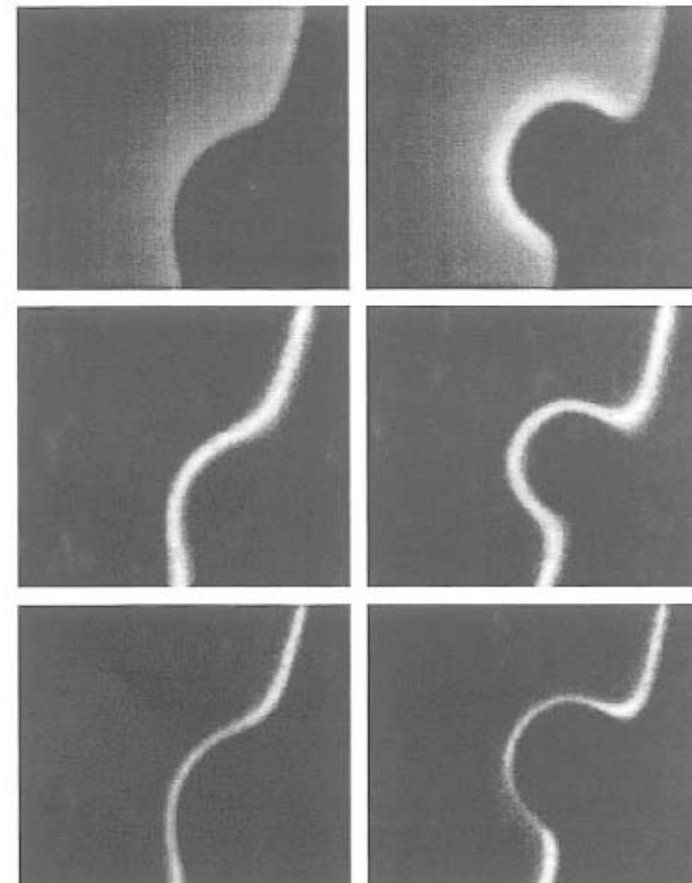


FIG. 3. PLIF images of OH (top), CH₂O (middle), and the product (bottom) taken at 2 ms (left) and 6 ms (right) into the interaction of a line-vortex pair with a laminar V-flame. Field of view 20 by 17 mm. The color table is linear running from black (low) to white (high signal).

[CH₂O][OH] imaging

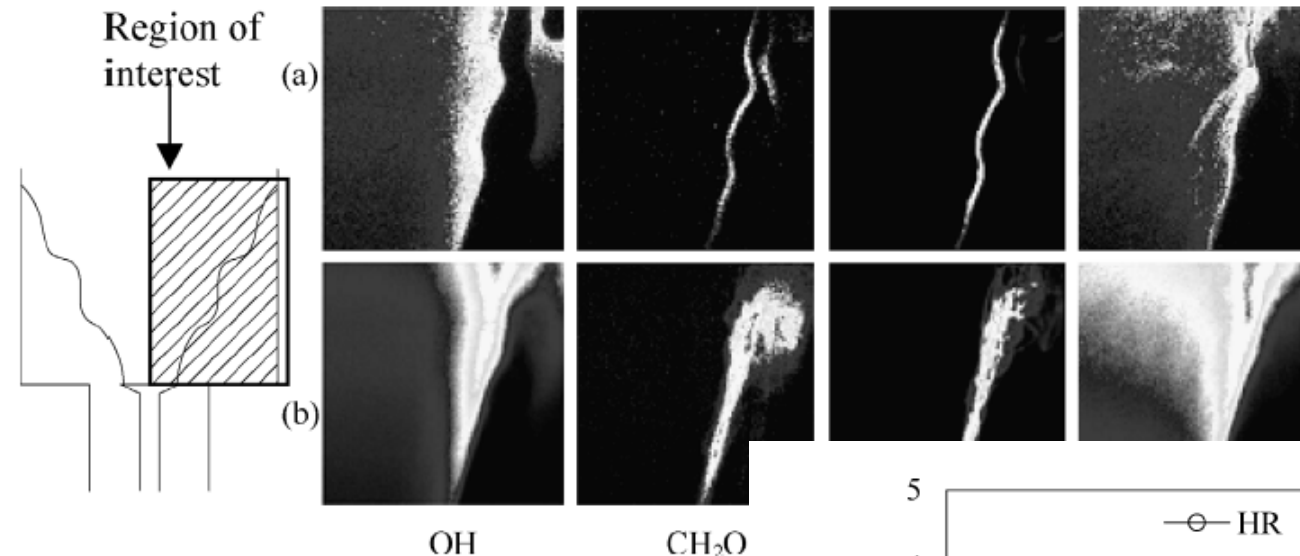


Fig. 9. (a) Images of OH PLIF, CH₂O PLIF, and corresponding HR and stabilized flame at $\phi = 0.6$. (b) Averaged OH PLIF, CH₂O PLIF, HR, and stabilized flame at $\phi = 0.6$.

Ayoola et al, Combustion and Flame 144 (2006) 1–16

Quantitative measurements
Low sensitivity to strain
Requires substantial effort
Sensitive to equivalence ratio fluctuations

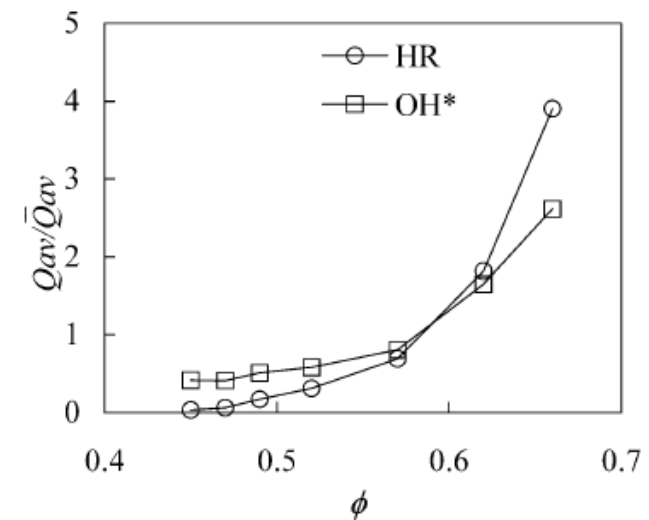
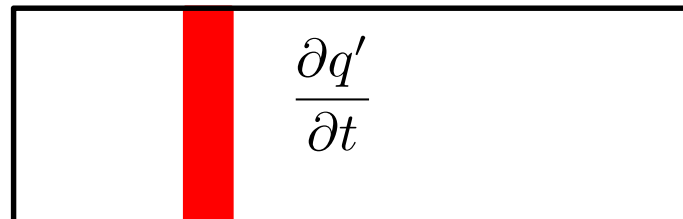


Fig. 10. Profiles of normalized HR and OH* in a bluff-body stabilized flame at different equivalence ratios.

Measurement of heat release rate fluctuation



- Direct
- Chemiluminescence
 - Premixed flames
 - ϕ oscillations
 - ϕ imaging
- Pressure

Chemiluminescence

Spectroscopic studies of low-pressure flames; temperature measurements in acetylene flames

BY A. G. GAYDON AND H. G. WOLFHARD, *Imperial College, London*

(Communicated by Sir Alfred Egerton, F.R.S.—Received 9 January 1948)

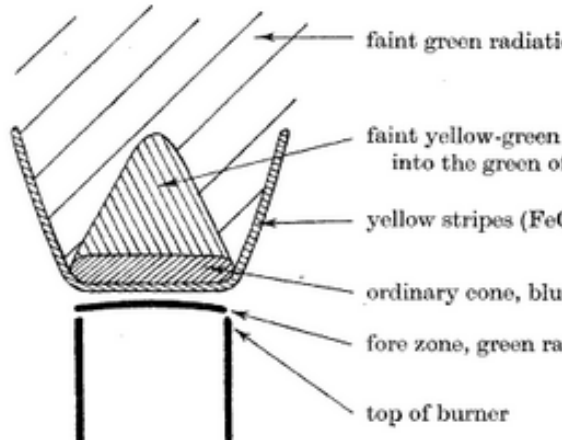
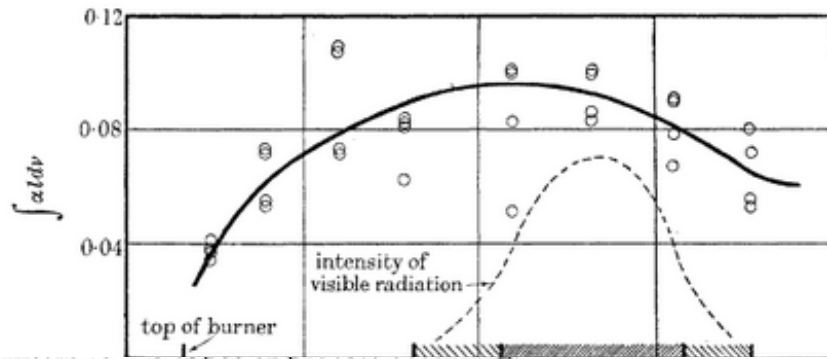


FIGURE 1. Flame coloured with

The experimental arrange

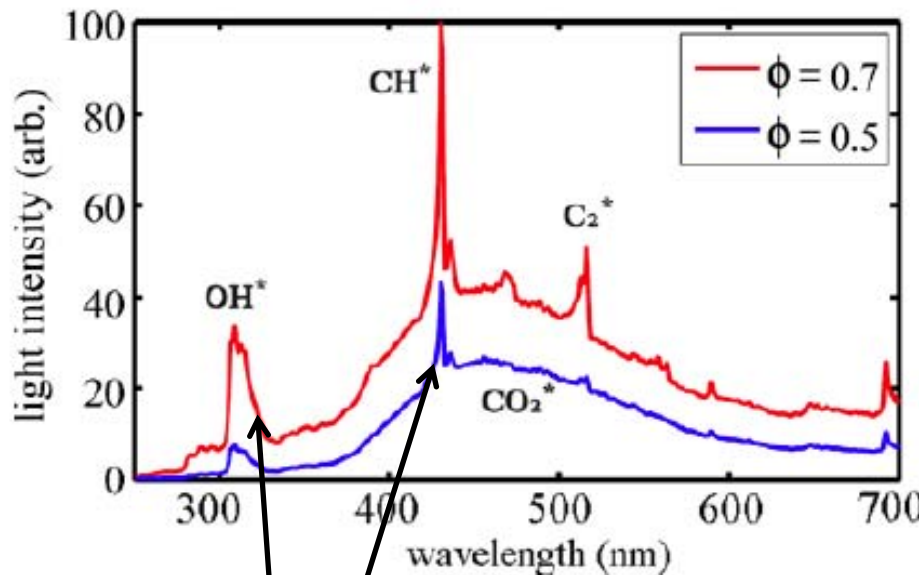


All these spectroscopic methods of measuring the temperature appear to give values which are much too high. This might appear to indicate that the flame contains some active species, such as for example an abnormally high concentration of fast electrons, which cause strong excitation of all substances in the flame. However, this is not supported by the observation that all the Fe lines do not reverse at the same temperature, or the fact that the rotational temperatures are in general higher than the excitation temperatures. Thus in the low-pressure flame of acetylene with air we have,

Theoretical flame temperature	2400° K
Excitation temperature by Fe lines	3500° K
Excitation temperature of OH	< 3800° K
Rotational temperature excited OH	5700° K

On the other hand, the temperature of the unexcited OH radicals (observed by absorption) probably does not differ much from the theoretical equilibrium value. It seems fairly certain that in these flames with acetylene the excitation of the OH is due to chemiluminescence. This is shown by the great strength of the OH radiation from these flames; it is around 500 times greater than from an oxy-hydrogen flame which has a comparable temperature and OH concentration. Also the OH radiation is vastly stronger in the reaction zone than just above, where the radiation is no doubt mainly thermal in origin.

Typical chemiluminescence spectra: premixed



Guethé, F., D. Guyot, G. Singla, N. Noiray, B. Schuermans,
Chemiluminescence as diagnostic tool in the development of gas
turbines, *Appl. Phys. B Lasers Opt.* (2012) 1–18.

Distinct lines

Lines subsumed by
luminescence

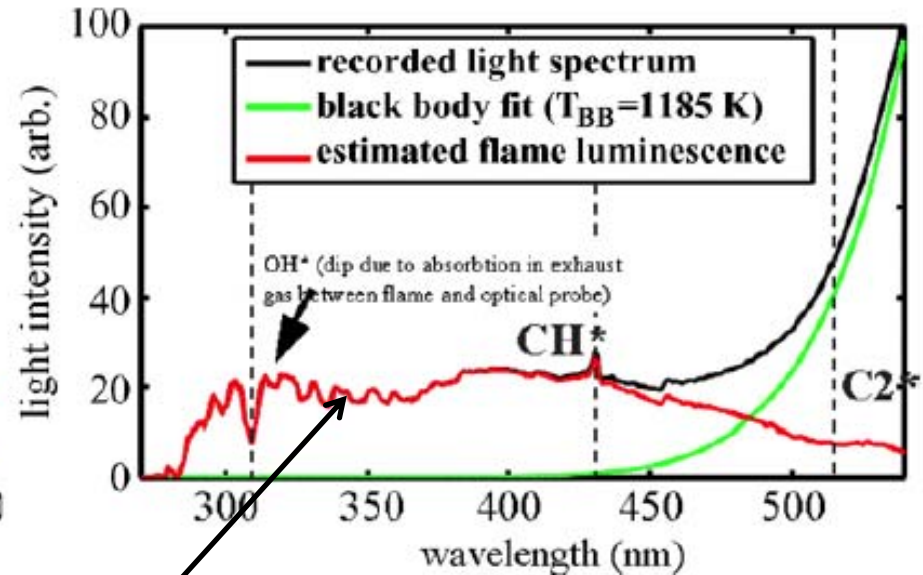


Fig. 1 Chemiluminescence spectra of swirl stabilised premix lab burners at atmospheric (*left*) and elevated gas turbine (> 15 bar) pressure (*right*) [32]

Chemiluminescence mechanisms

CH*:



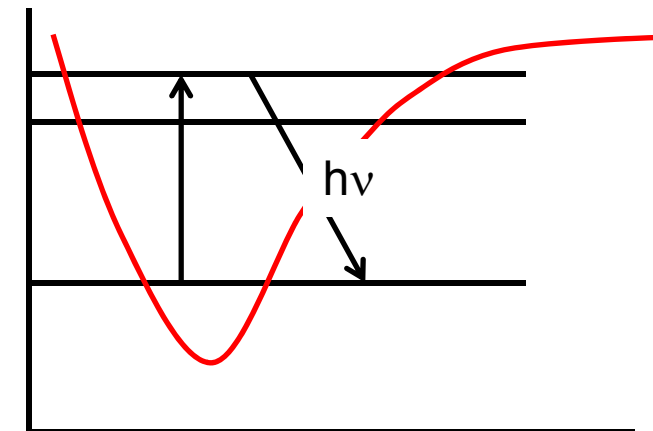
Small molecules

- energy does not accommodate in bonds
- energy levels compatible with visible range

OH*:



CO₂*:



CH*/OH* ratio, stoichiometry and power

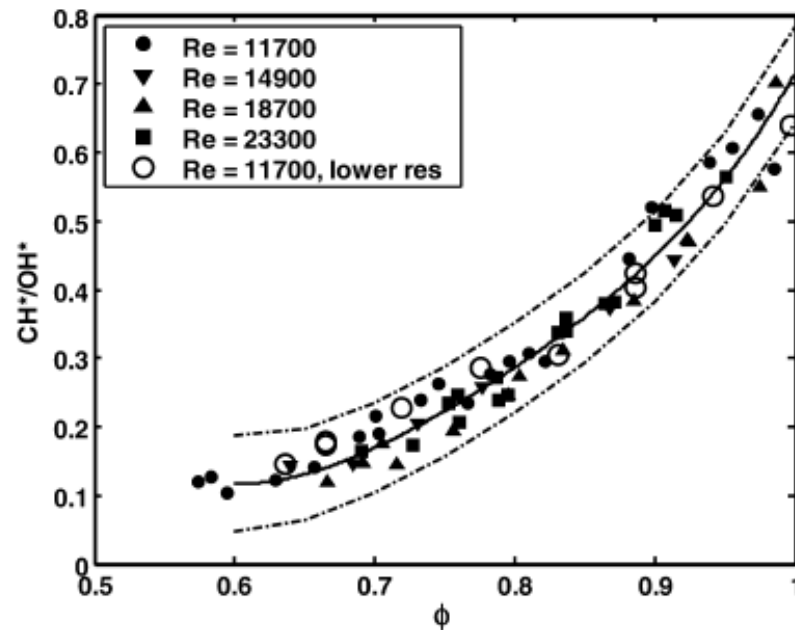


Fig. 3. Dependence of CH^*/OH^* on equivalence ratio for various inlet axial Re in the swirl combustor (solid line: 4th order least-square fit, dashed: 95% confidence).

Muruganandam, T.M., B.-H. Kim, M.R. Morrell, V. Nori, M. Patel, B.W. Romig, et al., Optical equivalence ratio sensors for gas turbine combustors, Proc. Combust. Inst. 30 (2005) 1601–1609.

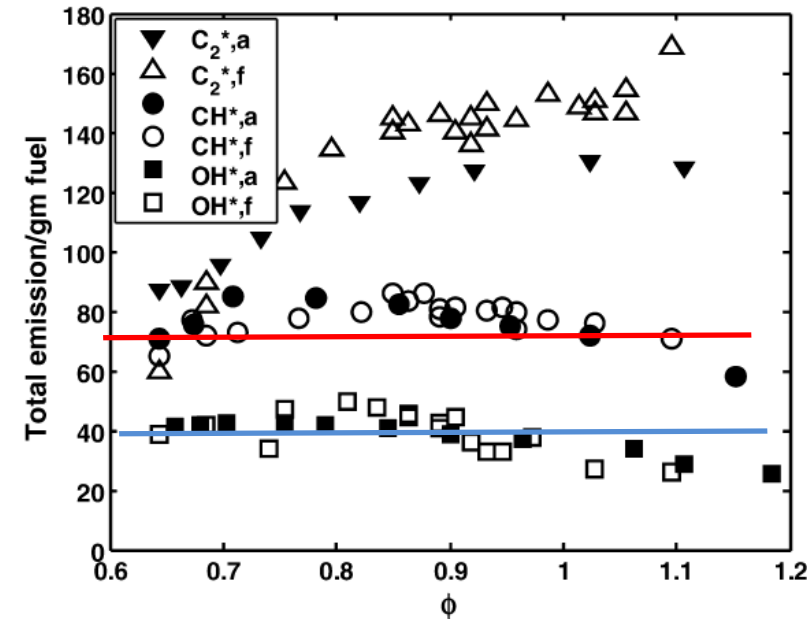


Fig. 6. Volume integrated chemiluminescence in the liquid fuel combustor (*n*-heptane) ($f = \phi$ varied by adjusting fuel, $a = \text{air adjusted}$).

- Premixed flames: CH^*/OH^* ratio scales with ϕ
- Total CH^* , OH^* chemiluminescence scales with power
- Partially mixed flames: ?

Localized measurements of CH*/OH*

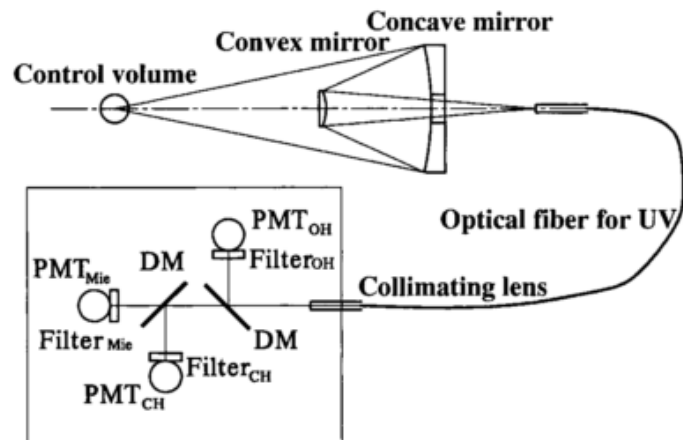
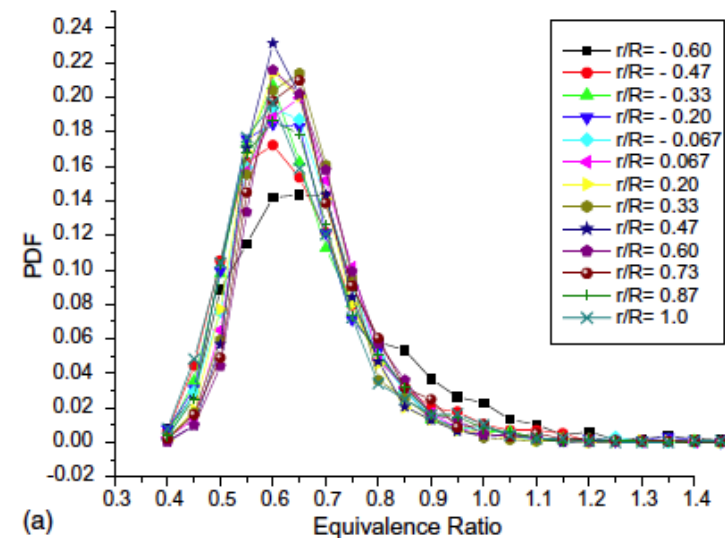
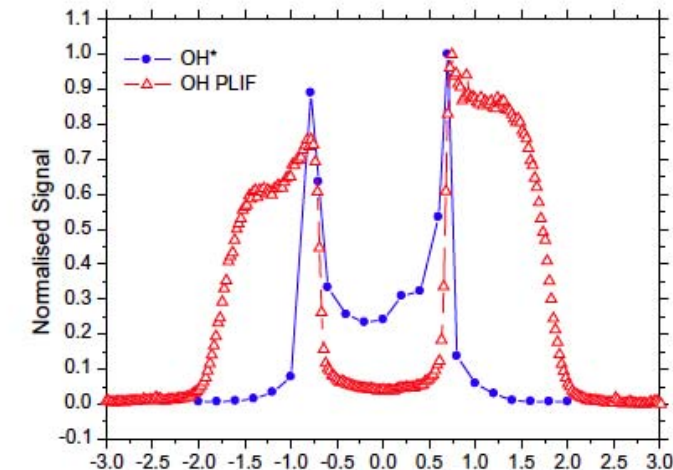


Figure 6. The light-detection system of MICRO.

Akamatsu, F., T. Wakabayashi, S. Tsushima, M. Katsuki, Y. Mizutani, Y. Ikeda, et al., The development of a light-collecting probe with high spatial resolution applicable to randomly fluctuating combustion fields, Meas. Sci. Technol. 10 (1999) 1240–1246 doi:10.1088/0957-0233/10/12/316.

Hardalupas, Y., M. Orain, C. S. Panoutsos, a. M.K.. Taylor, J. Olofsson, H. Seyfried, et al., Chemiluminescence sensor for local equivalence ratio of reacting mixtures of fuel and air (FLAMESEEK), Appl. Therm. Eng. 24 (2004) 1619–1632 doi:10.1016/j.applthermaleng.2003.10.028.



CO₂* background and pressure

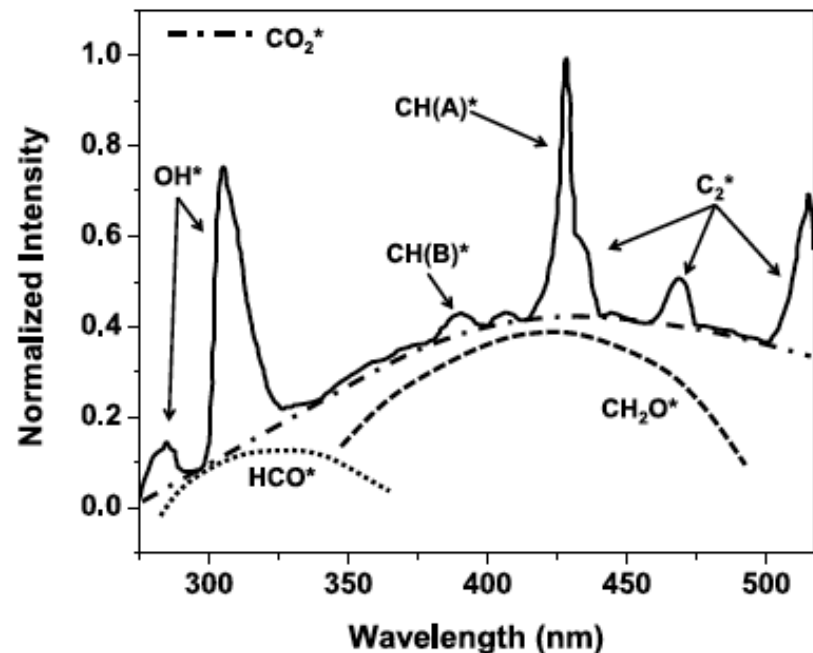


Fig. 1 Recreation of chemiluminescence spectrum showing the broad band background of the hydrocarbon chemiluminescence from CO₂^{*}, HCO^{*}, and CH₂O^{*}, based on work from [2, 3, 5, 6, 14]. Note that this portion does not cover the entire range of CO₂^{*} emission as suggested by [14]

Kopp, M., M. Brower, O. Mathieu, E. Petersen, F. Güthe, CO₂^{*} chemiluminescence study at low and elevated pressures, *Appl. Phys. B Lasers Opt.* 1-10 (2012) DOI 10.1007/s00340-012-5051-4.

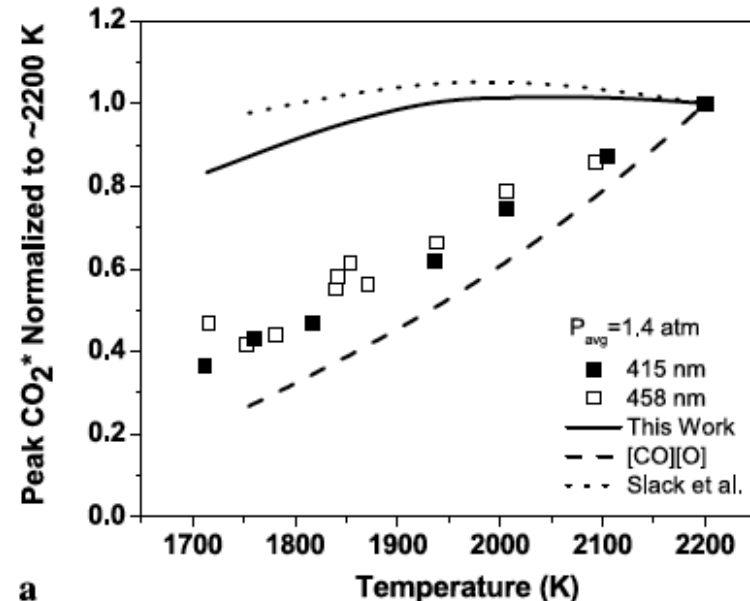


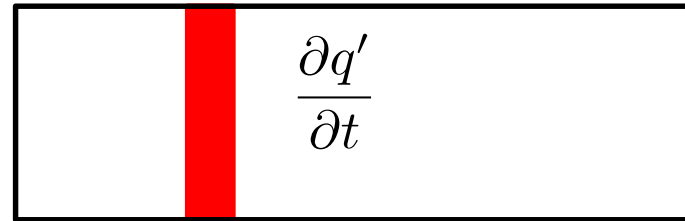
Fig. 10 Alternate peak CO₂^{*} predictions from another rate in the literature and experimental results from this work for average pressures of (a) 1.4 atm a

Mechanisms for CO₂^{*} can yield good relative results for background

Correction for CO₂^{*} especially important for CH^{*} measurements

Measurement of heat release rate fluctuation

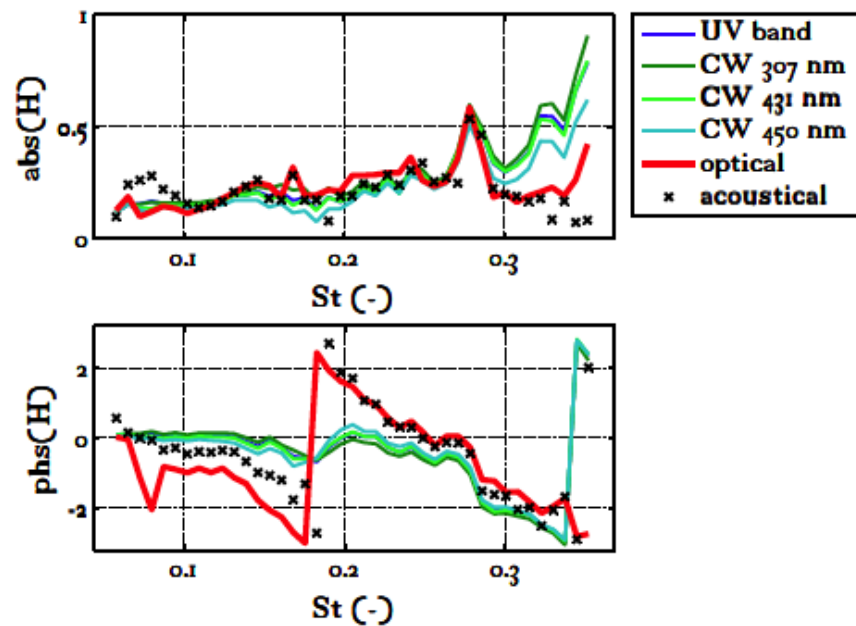
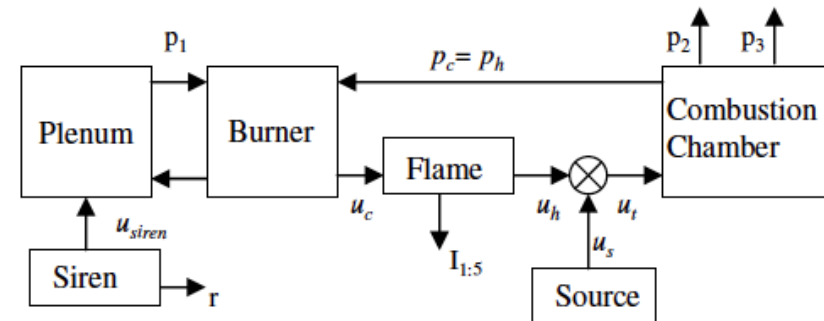
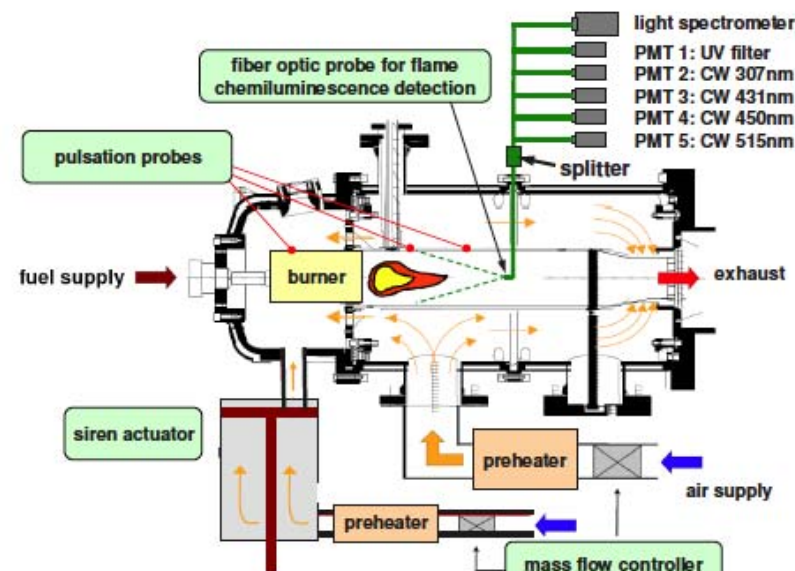




A diagram showing a flame front represented by a rectangle divided into two vertical sections: a white section on the left and a red section on the right. To the right of the red section, the mathematical expression $\frac{\partial q'}{\partial t}$ is written.

- Direct
- Chemiluminescence
- Pressure

Pressure vs. optical



Schuermans, B., F. Guethe, D. Pennel, D. Guyot, Paschereit, O. Thermoacoustic modeling of a gas turbine using transfer functions measured at full engine pressures, in: Am. Soc. Mech. Eng. Int. Gas Turbine Institute, Turbo Expo IGTI, 2009: pp. GT2009-59605.

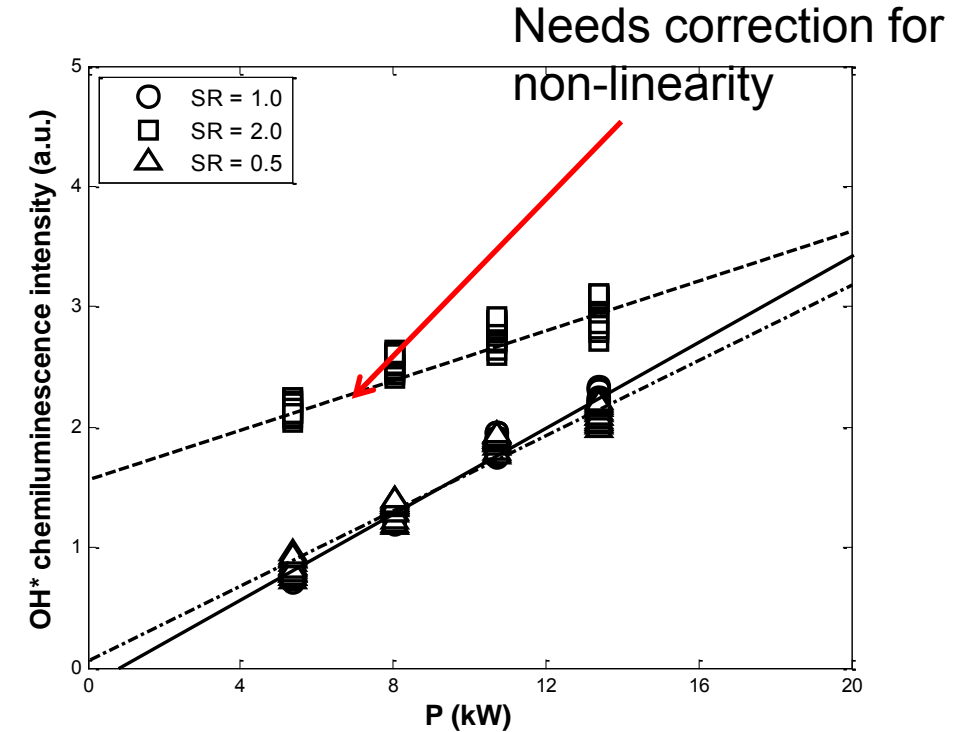
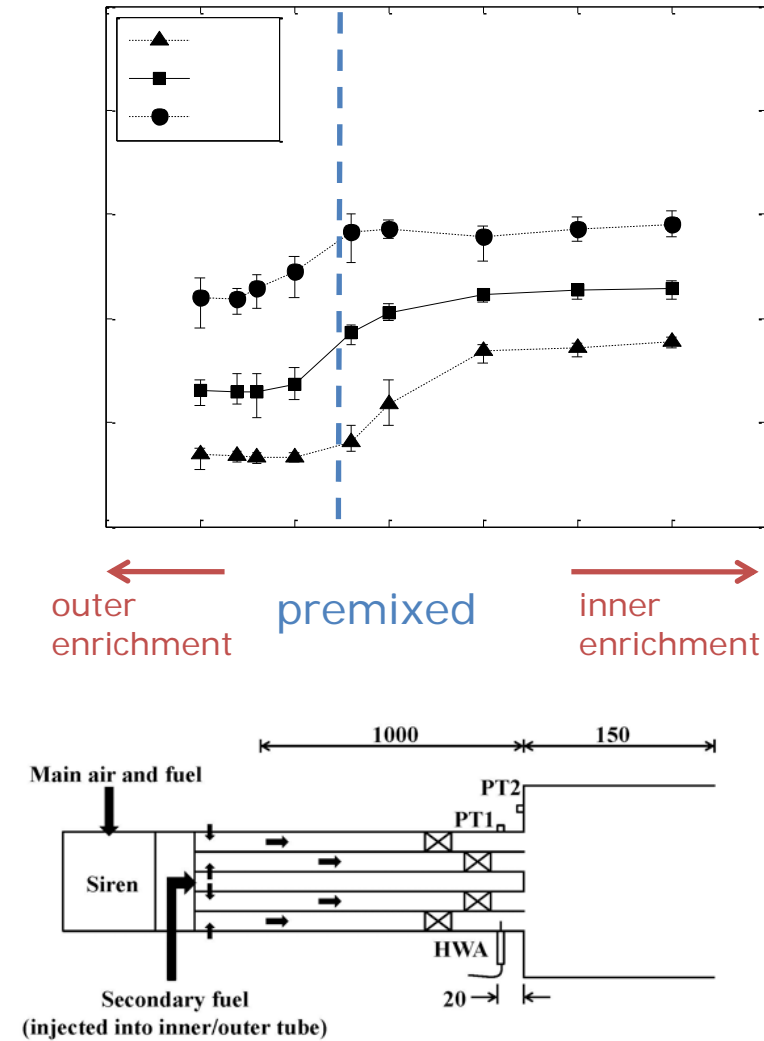
Schuermans, B., F. Guethe, W. Mohr, Optical Transfer Function Measurements for Technically Premixed Flames, J. Eng. Gas Turbines Power. 132 (2010) 081501 doi:10.1115/1.3124663.

Non-uniform equivalence ratio



Heat release rate correlations and equivalence ratio distribution

Han & Hochgreb, ECM 2013



Mean CH^* , OH^* varies with power
Slope varies with power
Ideally: calibration at fixed p , T , AFR, split

Equivalence ratio by line of sight absorption

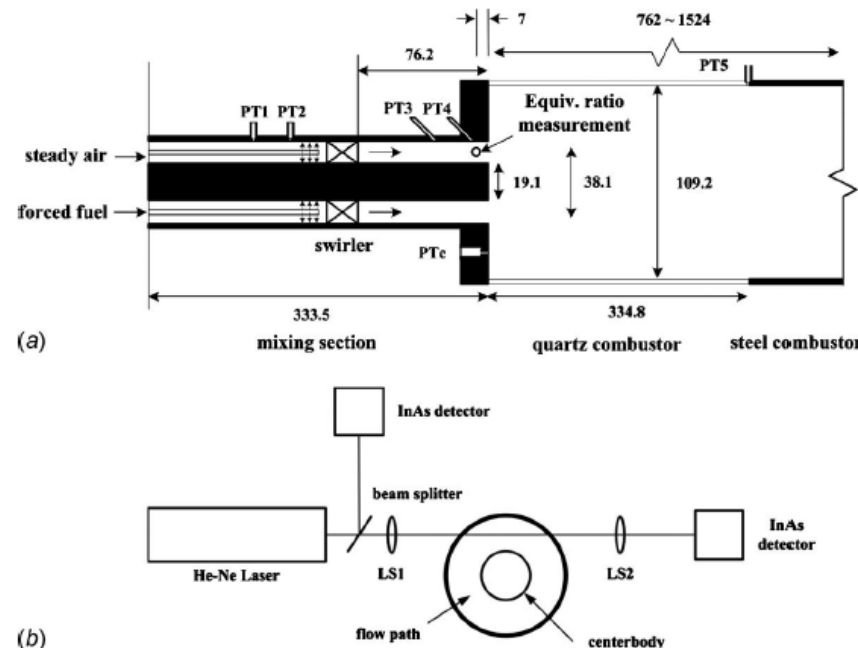


Fig. 2 Schematic of a swirl-stabilized, lean-premixed, gas turbine combustor. Dimensions in millimeters. (a) Side view (mixing section and quartz combustor section), (b) schematic drawing of experimental setup for equivalence ratio measurements.

Kim, K.T., J.G. Lee, B.D. Quay, D. Santavicca, Experimental Investigation of the Nonlinear Response of Swirl-Stabilized Flames to Equivalence Ratio Oscillations, *J. Eng. Gas Turbines Power*. 133 (2011) 021502 doi:10.1115/1.4001999.

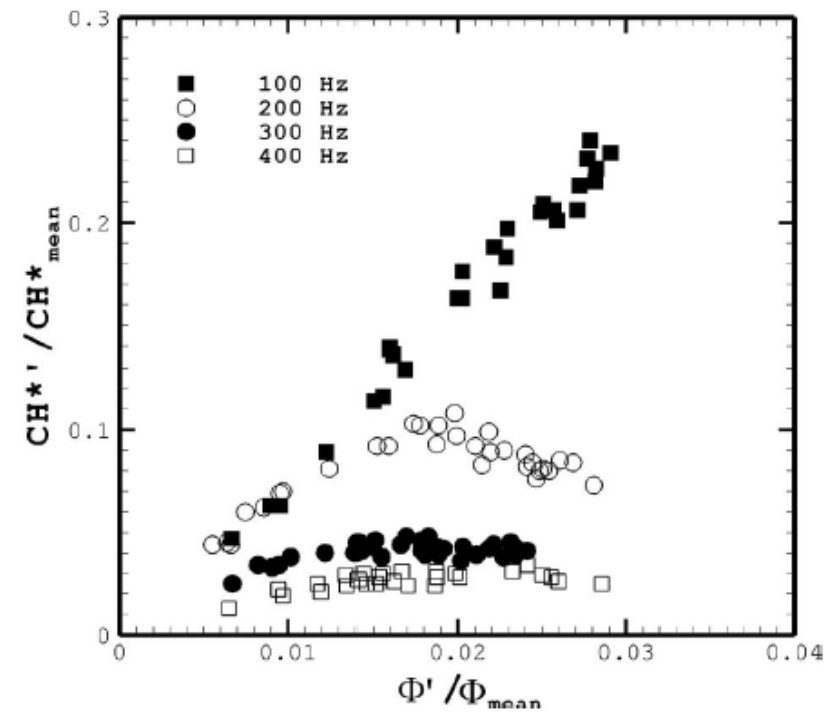
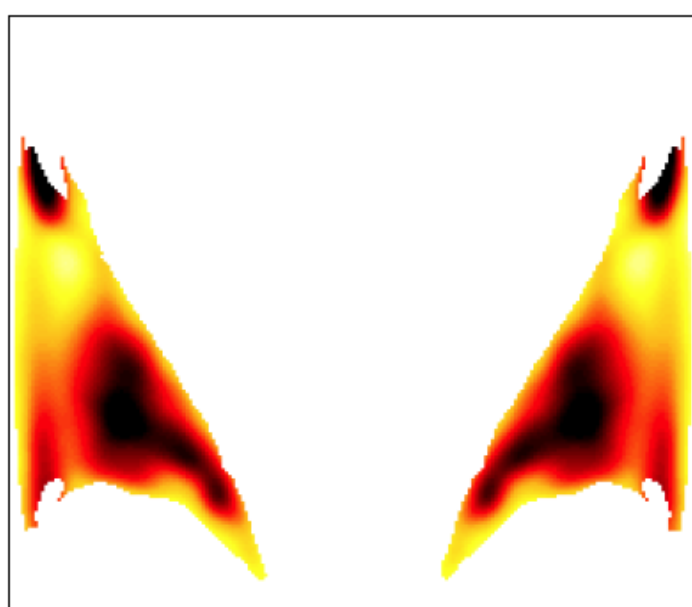


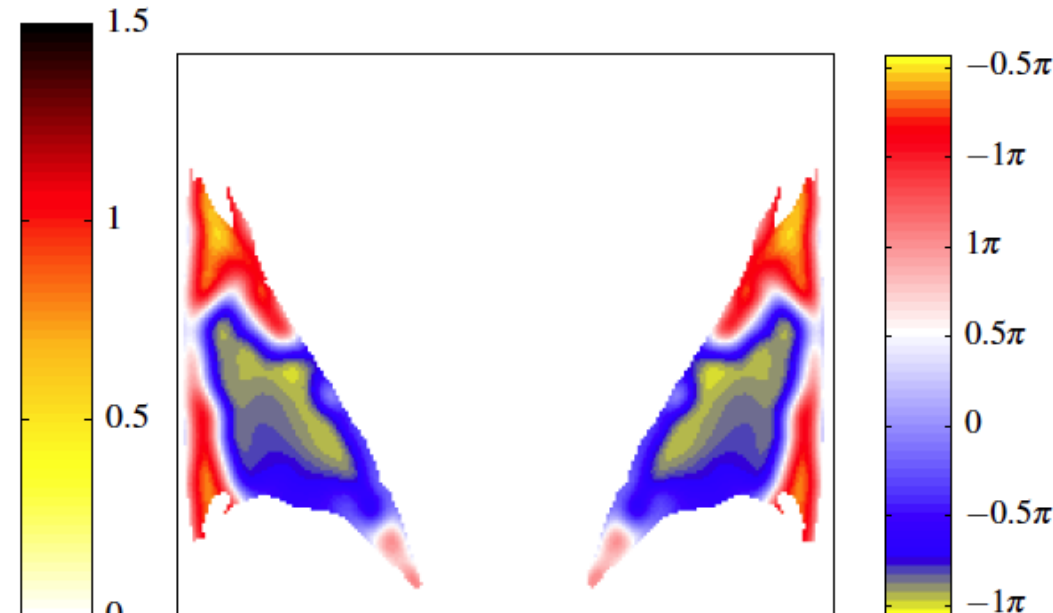
Fig. 6 Dependence of the normalized CH^* chemiluminescence intensity fluctuation on the modulation frequency. Inlet conditions: $T_{\text{in}}=200^\circ\text{C}$, $V_{\text{mean}}=60$ m/s, and $\Phi_{\text{mean}}=0.60$.

Φ from absorption measurements

$\text{CH}^*/\text{CO}_2^*$ ratio



(a) AMPLITUDE



(b) PHASE

Bobusch, B., Cosic, B., J.P. Moeck, C.O. Paschereit, Optical measurement of local and global transfer functions for equivalence ratio fluctuations in a turbulent swirl flame, in: Proc. ASME Turbo Expo 2013 Turbine Tech. Conf. Expo. GT2013 June 3-7, 2013, San Antonio, Texas, USA, 2013: pp. GT2013-95649.

Under lean conditions:
 $\text{CH}^*/\text{CO}_2^* \sim \text{C}/\text{O}_2$

Single camera method

Non-uniform flames: very much a project in development

Outline

- Measurement of heat release rates
 - Direct method
 - Chemiluminescence
 - Pressure method
- Imaging measurements
 - Chemiluminescence
 - OH PLIF
 - High speed measurements
 - Phase-reconstructed measurements

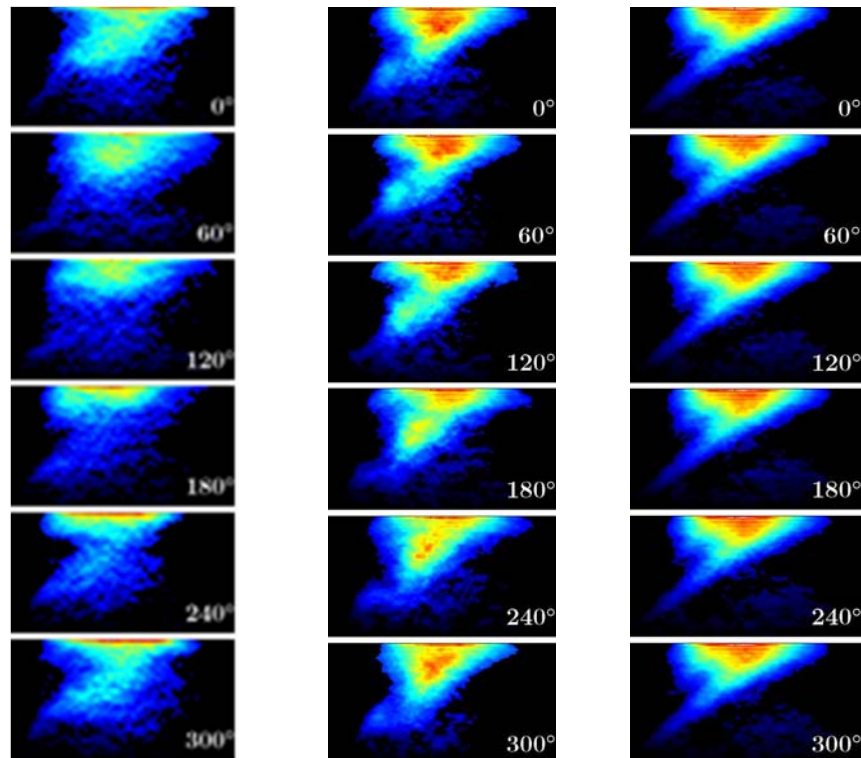
Measurable imaging dynamic quantities for instabilities



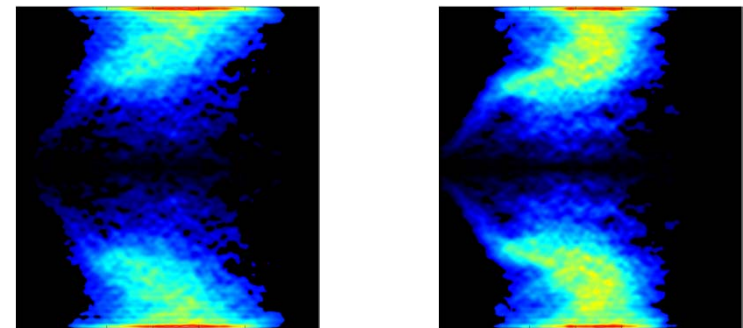
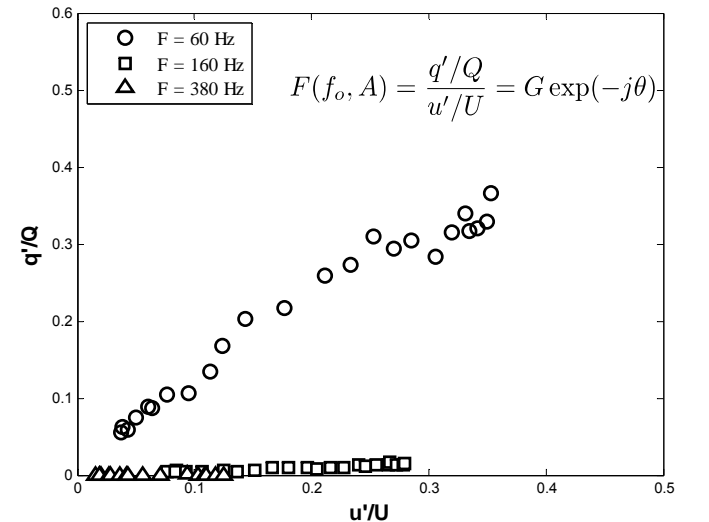
- OH*, CH*, CO₂*
 - Velocity (2D and 3D)
 - OH (HS-PLIF)
 - T (Rayleigh)
-
- HS CH, CH₂O PLIF feasible, but too low signal for current technologies

Flame behaviour - premixed

- $\Phi_g = 0.60$, $U = 5$ m/s, SR = 1.0
 $f_0 = 60, 160$ and 380 Hz



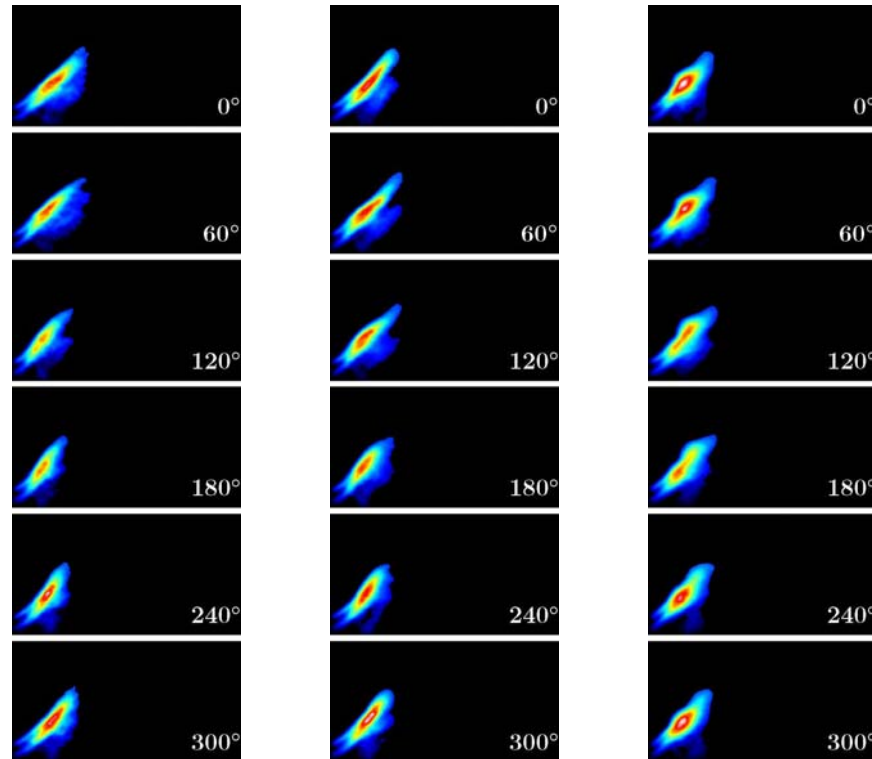
(a) $f_0 = 60$ Hz (b) $f_0 = 160$ Hz (c) $f_0 = 380$ Hz



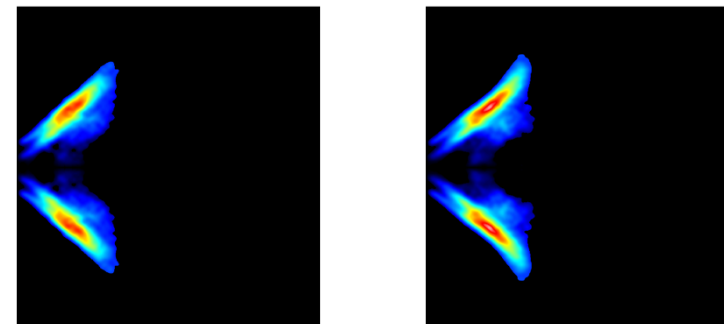
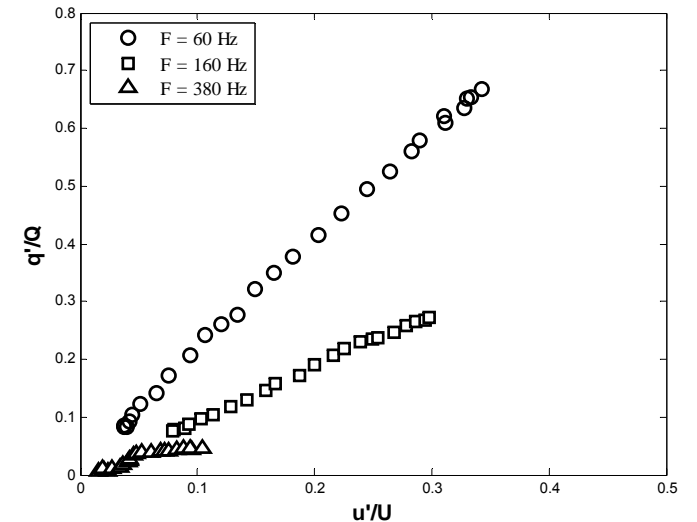
(1) $u'/U = 0.1$ (2) $u'/U = 0.2$
 $f_0 = 60$ Hz

Flame behaviour – SR = 2.0

- $\Phi_g = 0.60$, $U = 5$ m/s, SR = 2.0
 $f_0 = 60, 160$ and 380 Hz



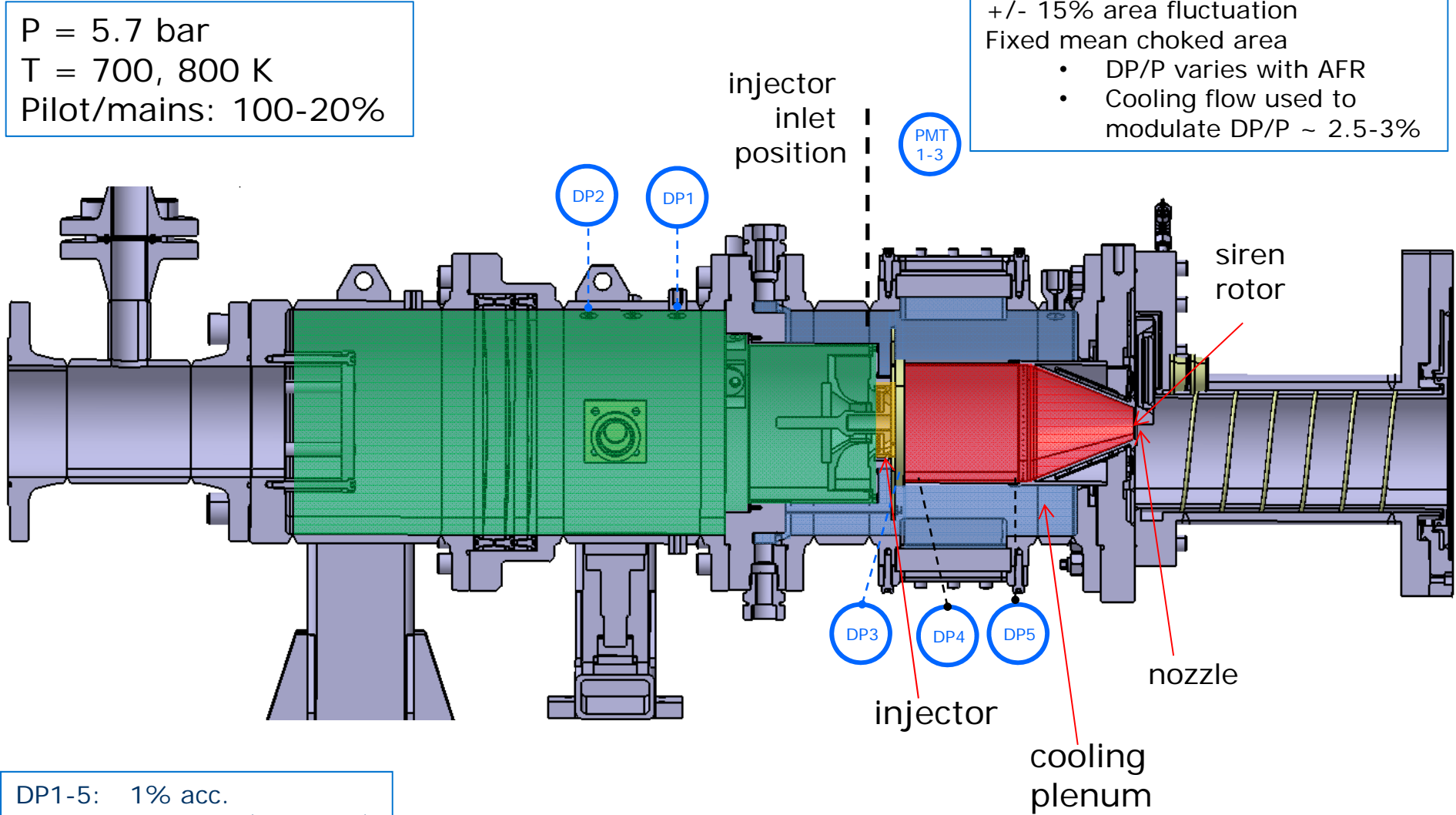
(a) $f_0 = 60$ Hz (b) $f_0 = 160$ Hz (c) $f_0 = 380$ Hz



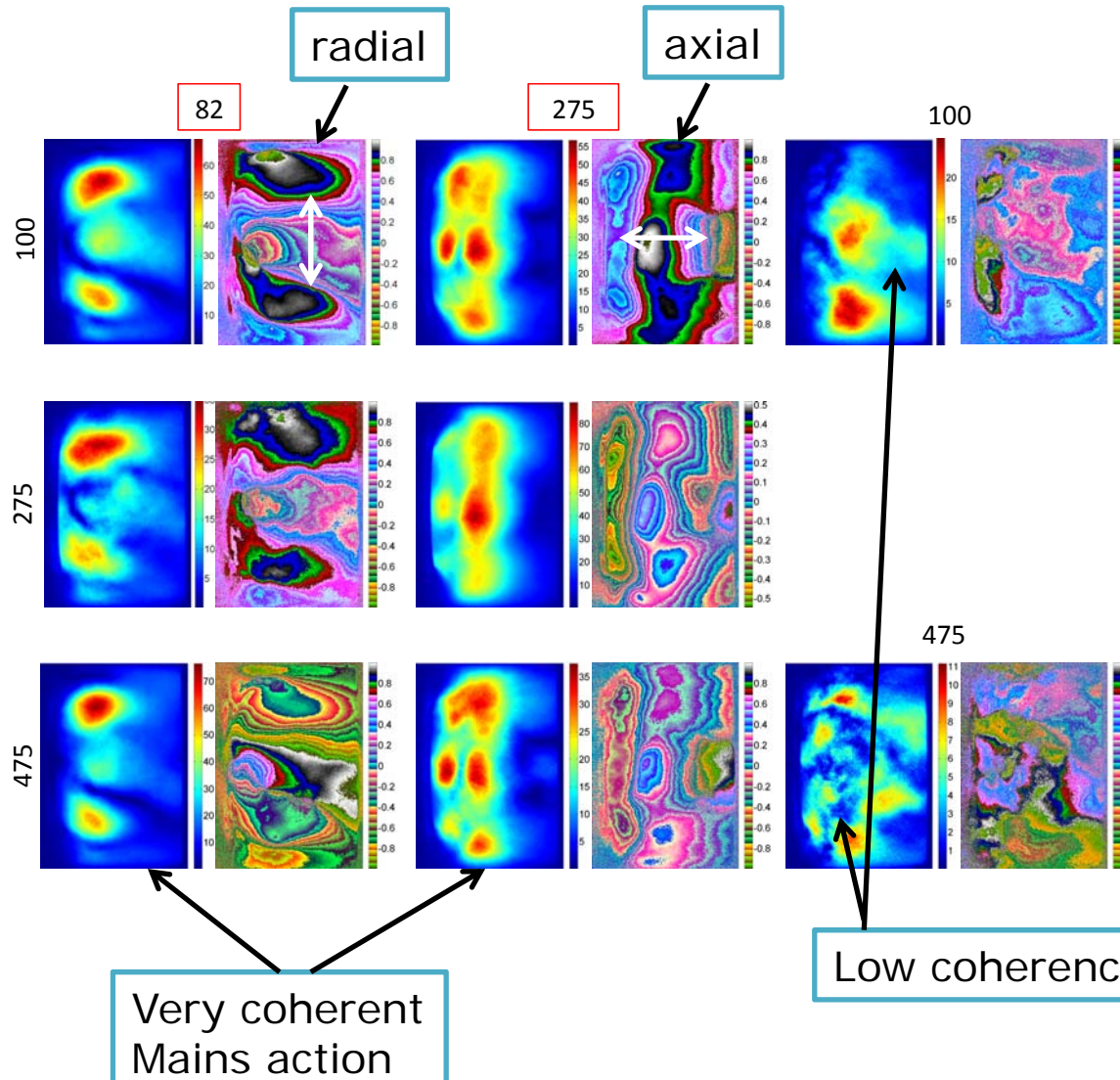
(1) $u'/U = 0.1$ (2) $u'/U = 0.2$
 $f_0 = 60$ Hz

CIPCF with siren

$P = 5.7$ bar
 $T = 700, 800$ K
Pilot/mains: 100-20%



HS OH* imaging: FFT amplitude and phase

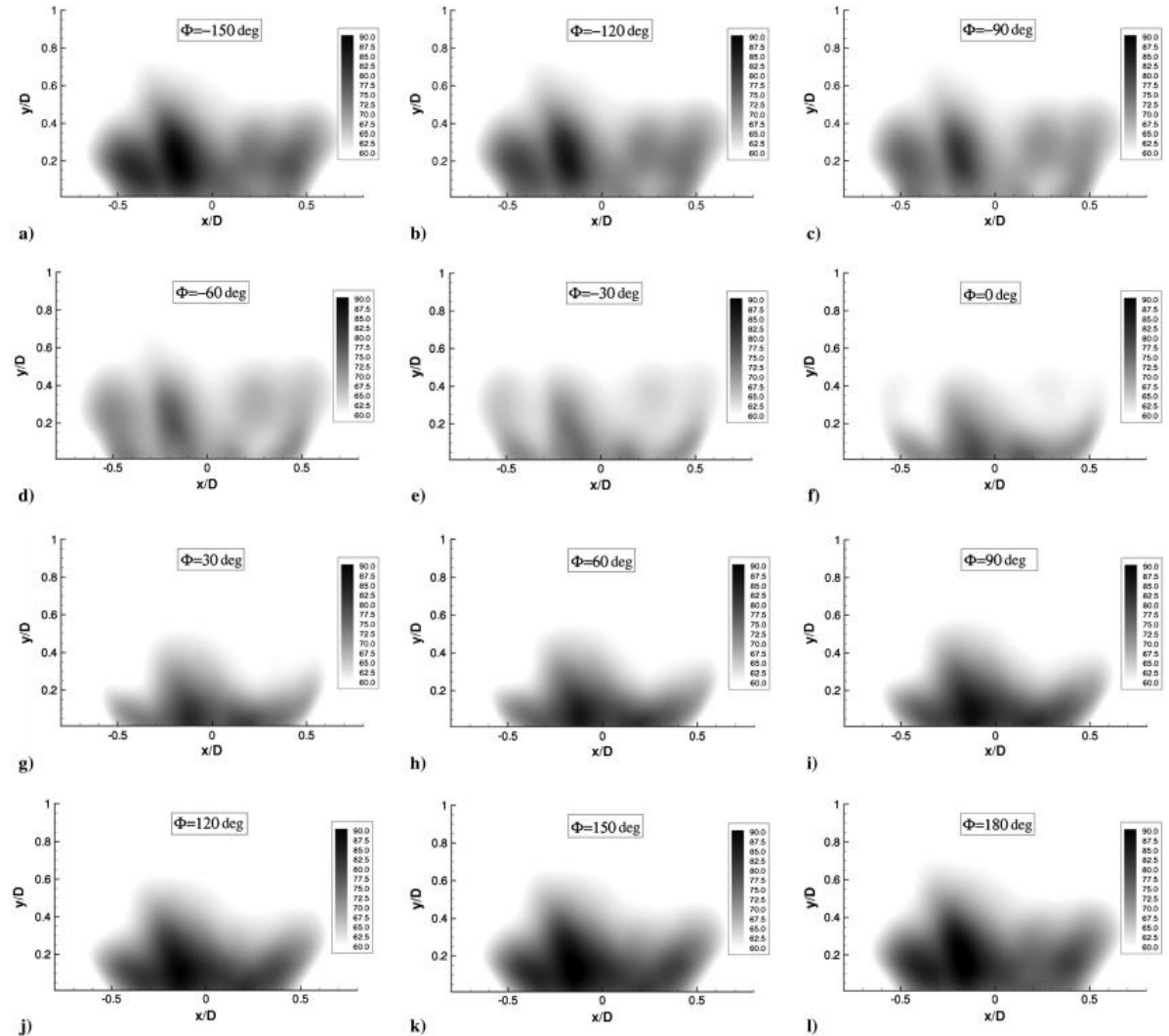


TP7
Kerosene
5.2 bar, 800 K
AFR 29
Split 20:80

Hochgreb, S, Dennis, D., Ayrancı,
I., Bainbridge, W. and Cant, R. S.,
ASME GT-2013-95311₃₀

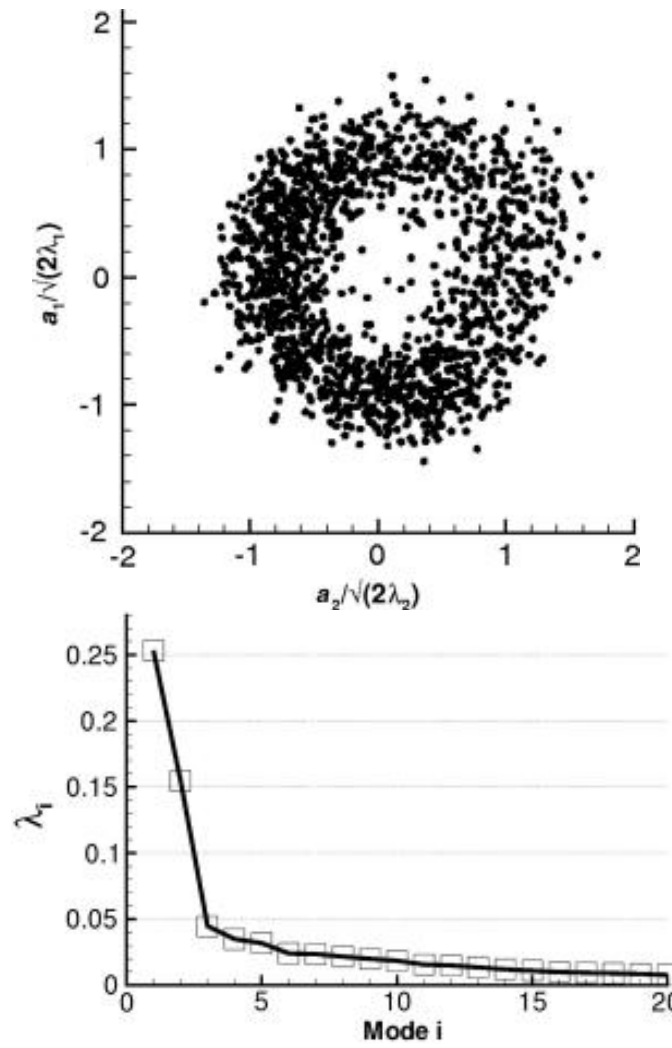
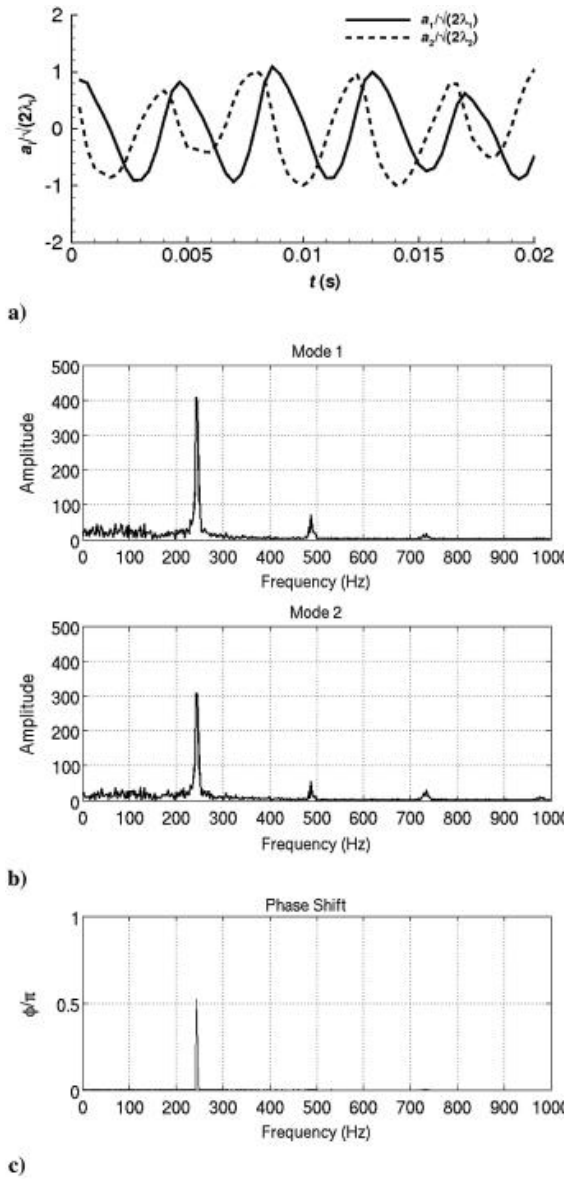
Proper Orthogonal Decomposition (POD) analysis OH* chemiluminescence

Iudiciani, P., C. Duwig, S.M. Husseini, R.Z. Szasz, L. Fuchs, E.J. Gutmark, Proper Orthogonal Decomposition for Experimental Investigation of Flame Instabilities, AIAA J. 50 (2012) 1843–1854
doi:10.2514/1.J051297.



TARS injector

POD decomposition OH*



Two main modes
separated by a phase
difference

HS PIV + OH PLIF during instabilities

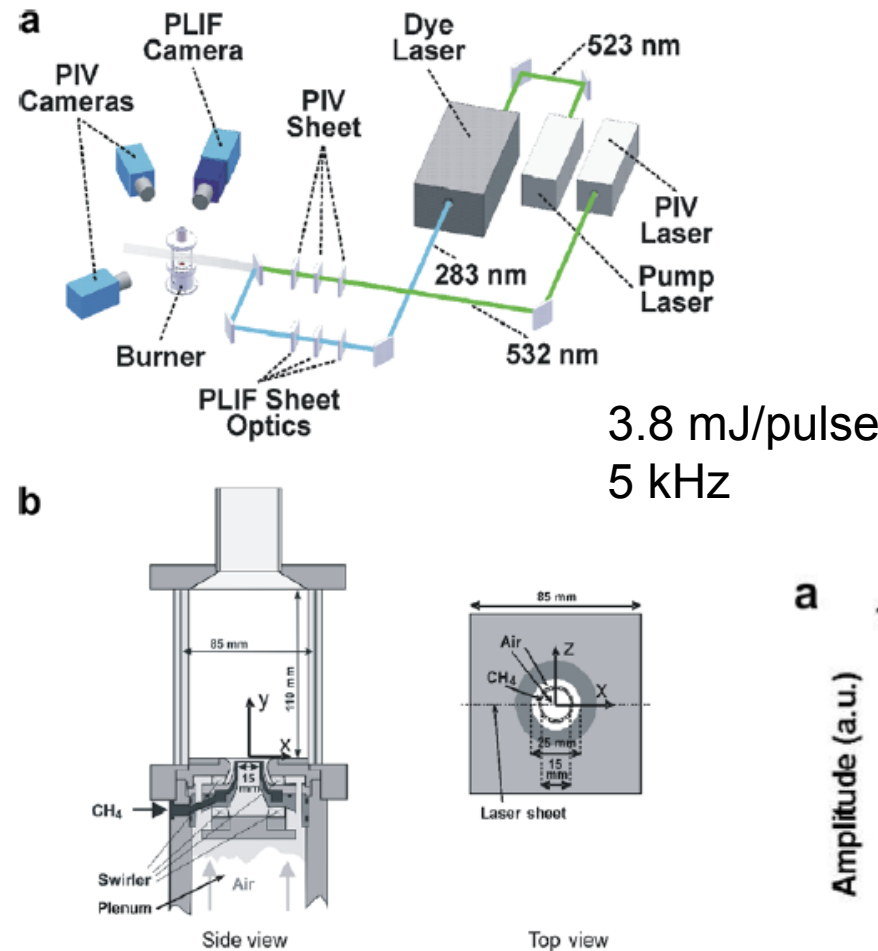


Fig. 1. (a) Experiment configuration. (b) Dual-swirl GTMC burner.

I. Boxx et al., Combust. Flame (2010),
doi:10.1016/j.combustflame.2009.12.015

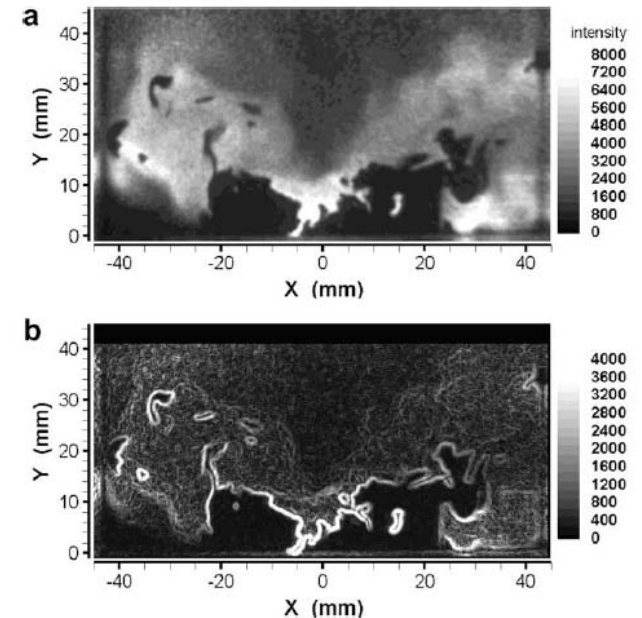
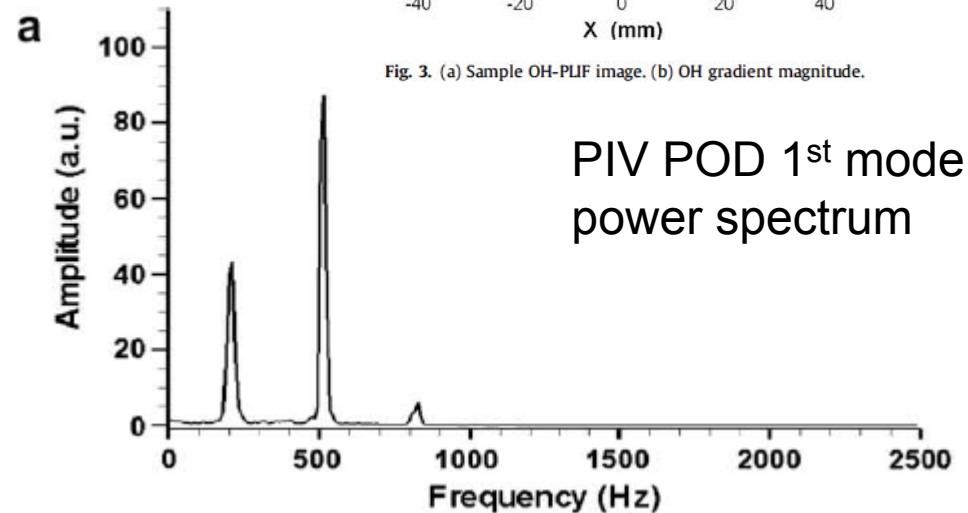
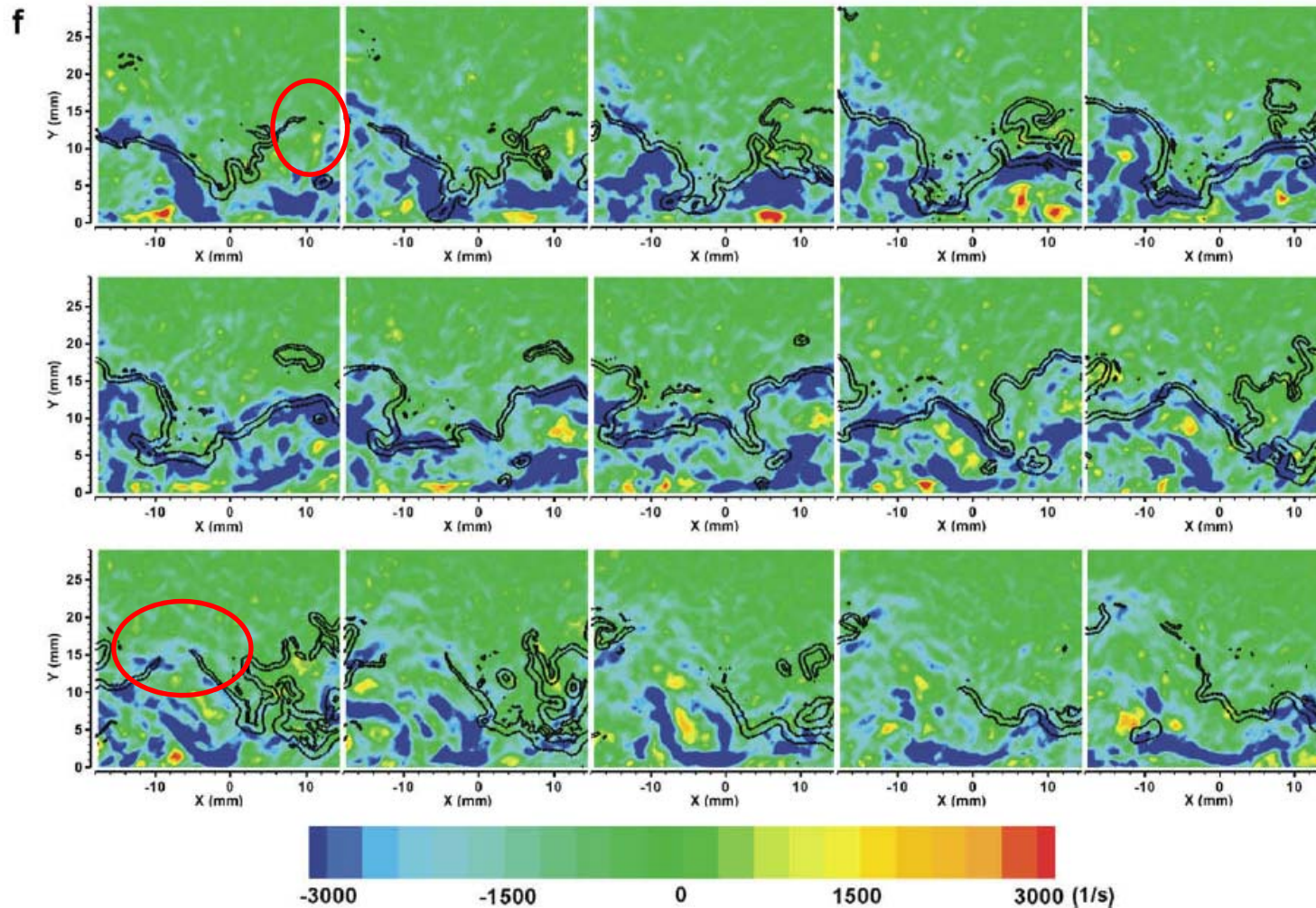


Fig. 3. (a) Sample OH-PLIF image. (b) OH gradient magnitude.



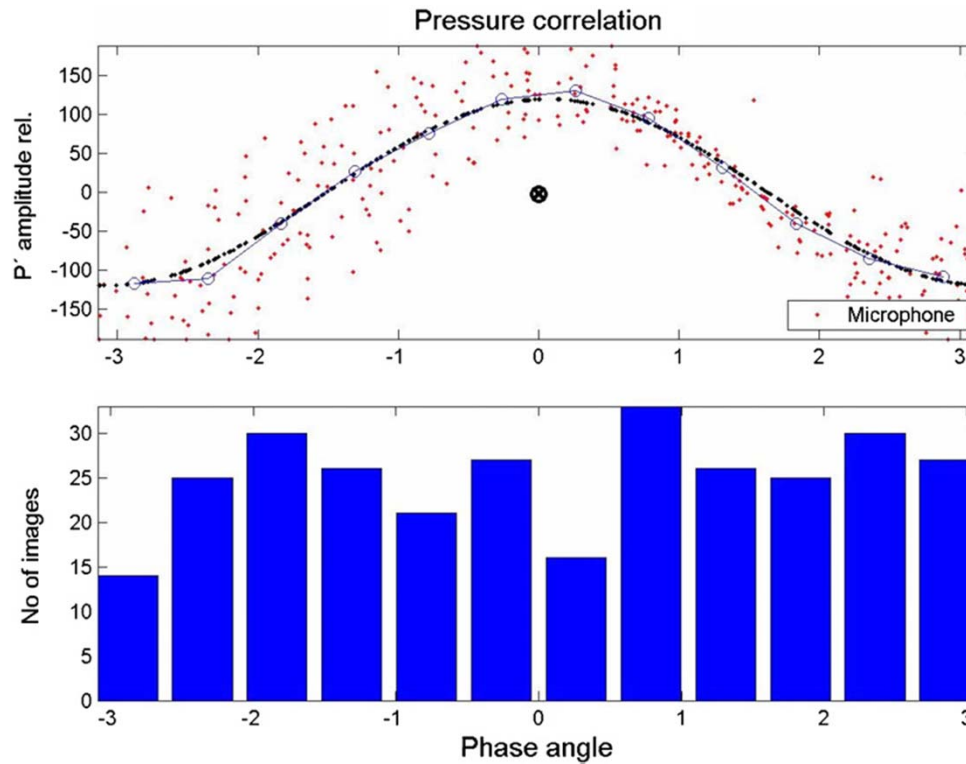
PIV POD 1st mode power spectrum

Reaction zones and min principal strain rate



I. Boxx et al., Combust. Flame (2010),
doi:10.1016/j.combustflame.2009.12.015

Phase-locking from discrete (non-high speed) images with random cycle



Hilbert transform

$$C(t_p) = \mathcal{F}^{-1} [\mathcal{F}[p(t_p)]H(f_{qN} - f_q)]$$

Güthe, F., B. Schuermans, Phase-locking in post-processing for pulsating flames, Meas. Sci. Technol. 18 (2007) 3036–3042
doi:10.1088/0957-0233/18/9/039.

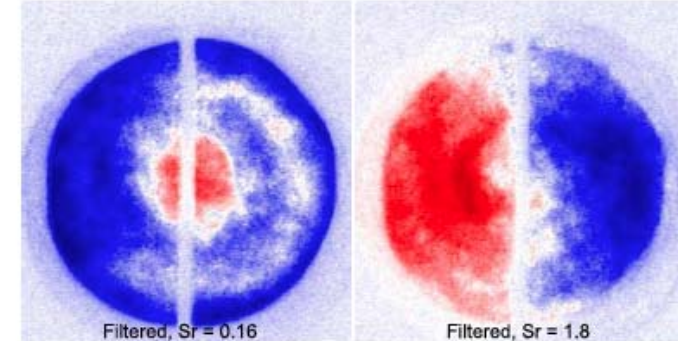


Figure 10. Rayleigh plot from filtered pressure function locked to frequency $Sr = 0.16$ (left) and $Sr = 1.8$ (right).

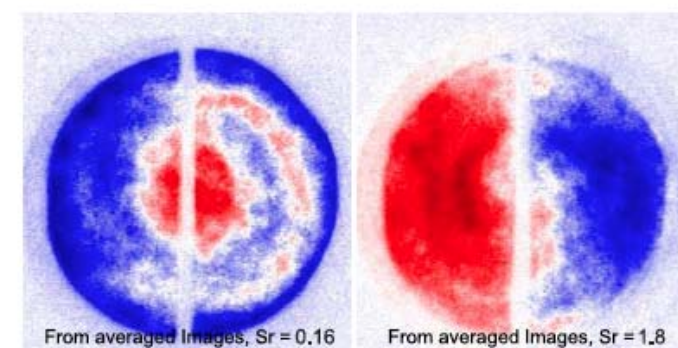


Figure 11. Rayleigh plot from phase averaged images locked to the frequency $Sr = 0.16$ (left) and $Sr = 1.8$ (right) using an idealized cosine function for the pressure.

Equivalent to a narrow local f filter

- Chemiluminescence:
 - Simple, inexpensive and fast
 - Quantitative (with appropriate calibration)
 - Questionable for partially mixed systems
- Imaging
 - High speed dynamic PIV, OH PLIF possible, additional insight: but cumbersome, expensive.
 - Low speed phase reconstruction possible via Hilbert transforms: high quality imaging and phase discrimination, but more labor intensive
 - Interpretation of large quantities of information still difficult: low order reduction techniques (POD, DMD) evolving and important → experimenters learning from computational researchers